Hindawi
Adsorption Science & Technology
Volume 2022, Article ID 7701128, 13 pages
https://doi.org/10.1155/2022/7701128

*Research Article*

# Synthesis and Characterization of Activated Carbon from Agrowastes for the Removal of Acetic Acid from an Aqueous Solution

**Joel Brian Njewa**,[1,2] **Timothy Tiwonge Biswick**,[1] **Ephraim Vunain**,[1] **Cheruiyot Silas Lagat**,[2] **and Solomon Omwoma Lugasi**[2]

[1]*University of Malawi, Department of Chemistry, P.O. Box 280, Zomba, Malawi*
[2]*Jaramogi Oginga Odinga University of Science and Technology, Department of Physical Science, P.O. Box 210-40601, Bondo, Kenya*

Correspondence should be addressed to Joel Brian Njewa; njewajoel@gmail.com

Received 13 January 2022; Revised 27 March 2022; Accepted 18 May 2022; Published 6 June 2022

Academic Editor: Eloy S. Sanz



In this study, activated carbons prepared from agrowastes by chemical activation were used to remove acetic acid from an aqueous solution through a batch process. The prepared adsorbents were characterized by SEM, XRD, FT-IR, and point of zero charge (pHpzc). The effects of adsorbent dosage, initial concentration, and contact time were considered. Equilibrium data was tested using Langmuir, Freundlich, Temkin, and Frenkel–Halsey–Hill models. The degree of adsorption of acetic acid increased for both adsorbents as contact time, and adsorbent dosage and initial concentration were increased. The adsorption data were described well by the (Freundlich=Frenkel–Halsey–Hill) models with the highest regression coefficient of $R^2 = 0.9961$ and $R^2 = 0.9951$ for Rice Husk Activated Carbon (RH-AC) and Potato Peels Activated Carbon (PP-AC), respectively. This suggests a multilayer through the existence of a heterogeneous pore distribution in the adsorbent surface. Kinetic data agreed well with pseudosecond-order ($R^2 = 0.999$ and $R^2 = 0.994$) RH-AC and PP-AC, correspondingly. This indicates that the adsorption process was chemisorption in nature. The regeneration studies showed that the adsorbents prepared could be renewed and reused before losing their adsorbing affinity for acetic acid.

## 1. Introduction

Manufacturing industries still remain the backbone of the economy in both developing and developed countries. However, of late, rapid industrial growth has resulted into disastrous environmental damage and pollution. Effluents originating from manufacturing industries flowing into water bodies have result into surface and groundwater pollution [1]. Studies done in Egypt and Malaysia, for example, have detected a large array of chemical pollutants of industrial origin exceeding the permissible limits for wastewater. Among wastewater pollutants are organic and inorganic chemicals, heavy metals, petrochemicals, chloroform, and bacteria [2–4]. Most of the organic pollutants normally experience an oxidation process producing carboxylic acids such as dicarboxylic acids as final products. Maleic, acetic, and oxalic acids are well-known examples of dicarboxylic acids. Research findings have shown that high levels of these acids in potable water result into despicable health problems to human beings such as kidney stones, uremia, corrosion of enamel and mouth, vomiting, and hematemesis, just to mention a few [5].

Acetic acid, in particular, is among the organic compounds recently reported in wastewater as a contaminant despite it being a key component very useful in various industrial processes such as the manufacturing of high-grade phosphate fertilizer, as a rust proofing agent of iron metals, and as baking powder as well as phosphate syrup used in soft drinks or as a water softening agent [1]. There are several techniques which are used in order to remove organic pollutants in water, main of which include the following: phytoremediation, bioremediation, reductive and

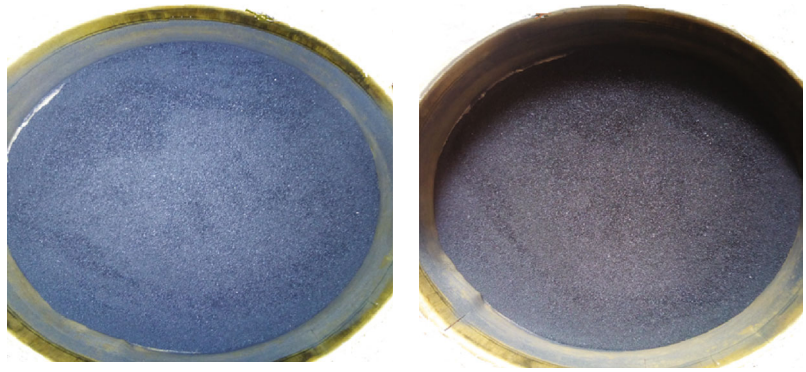

(a) (b)

Figure 1: Synthesized activated carbons (a) RH-AC and (b) PP-AC.

oxidative process, separation by membranes, liquid-liquid extraction, and adsorption [6]. Of all these processes, adsorption still remains the best and widely recognized method of purification for very good reasons. First, it is simple and easy to operate. Second, it is cheap and so far the most effective purification technique for various organic pollutants from water and wastewater. In addition, it has been observed to produce high-quality treated effluents [7–9]. On adsorbent materials, there are a variety of them such as silica gel, zeolites, synthetic adsorbents (resins), clays, activated alumina, and activated carbon which are used in the treatment processes of industrial wastewater containing chemical pollutants [10]. However, activated carbon is the most preferred adsorbent used to eliminate harmful chemical compounds from wastewater including acetic acid at low concentrations [11]. This is due to its high adsorption efficiency, its porous structure, and the presence of high surface area [12].

Generally, carbonaceous materials are typically prepared from materials rich in elemental carbon such as petroleum residues, peat, fossil coals, lignite, and coke, all of which are highly costly and nonrenewable [13]. As an alternative, investigators have successfully prepared affordable activated carbons from various sources of agrowastes [14–16].

There are two routes which can be adopted for synthesizing activated carbon for wastewater treatment, namely, physical and chemical. Physical activation starts with carbonization of the materials at elevated temperatures ranging from 500°C to 900°C in an inert atmosphere. The carbonized material is then activated by subjecting it to oxidative gases like carbon dioxide, oxygen, and nitrogen at temperatures ranging from 800°C to 1000°C [17]. The first step is performed to remove noncarbon elements while the final step is aimed at attaining surface porosity. Chemical activation, on the other hand, combines carbonization and activation into a single step, with the raw material being impregnated with a chemical activating agent and then activated in an inert atmosphere [18]. Chemical activation enjoys more advantages over physical activation. These include a lower activation temperature, a larger carbon yield, and more porosity [19].

Various published reports indicate that some researchers have prepared excellent activated carbon adsorbents from agricultural by-products and have successfully used them for the removal of inorganic pollutants in aqueous solutions [20–23]. Currently, there are no published research findings that we are aware of that have reported the use of rice husks and Irish potato peels as carbonaceous materials for the elimination of organic contaminants specifically acetic acids. While emphasizing on the need to eliminate the undesirable health effects of industrial wastewater on human beings and in quest to meet the suitable requirements of effluent quality set by the Malawi Bureau of Standards and Environmental Regulatory Agency, this research, presents a groundbreaking discovery of the use of low-cost activated carbons prepared from agrowastes through chemical activation processes to remove acetic acid in an aqueous solution.

## 2. Materials and Methods

*2.1. Chemicals and Reagents.* All chemicals used were of analytical grade. The phosphoric acid ($H_3PO_4$), sodium hydroxide (NaOH), and hydrochloric acid (HCl) were supplied by Sigma Aldrich (Germany) while nitric acid, ($KNO_3$), and ethanoic acid ($CH_3COOH$) reagents were provided by Minema Chemicals (PTY) Ltd (South Africa). All required solutions were made by dissolving the corresponding reagent in double-distilled water.

*2.2. Source of Raw Materials.* The precursors (rice husks and Irish potato peels) were collected from Songani and Zomba Free Market in Zomba, Malawi. The precursors were firstly washed with running tap water until the color of the materials was clear and then were washed in deionized water to completely remove the remaining surface impurities. The precursors were sun-dried for a day and then oven-dried at a temperature of 80°C overnight. The dried samples were then ground using an electric blender and were sieved to obtain precursor powder of particle size less than 500 $\mu$m. The powders were kept in air-tight container pending use.

*2.3. Preparation of Adsorbents.* The activated carbons were successfully prepared through chemical activation using 40% orthophosphoric acid ($H_3PO_4$) as an activating agent (Figure 1). The impregnation ratio of 1 : 2 (solid/liquid) was adopted and then left in an electric oven at a

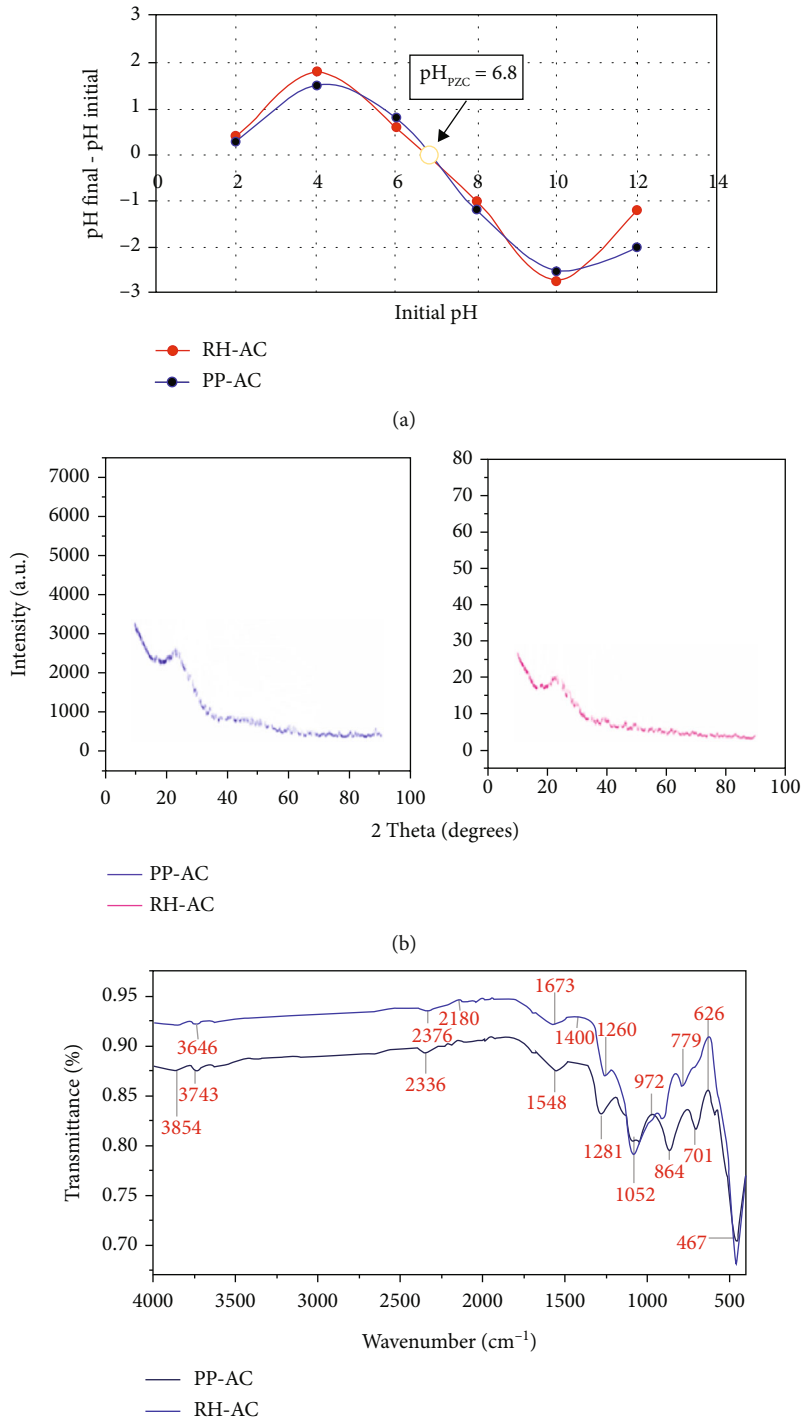


Figure 2: The (a) pHpzc for RH-AC and PP-AC, (b) X-ray chromatogram, and (c) FT-IR spectra.

temperature of 80°C for 12 h to ensure acid penetration into the interior pores and for water evaporation. The samples were then heated in a muffle furnace in the absence of air at the temperature of 500°C for 1.5 h. The samples were allowed to cool to room temperature in a desiccator and sequentially washed with 0.1 M NaOH, warm, and then cold water until the pH of the water was neutral. The samples were oven-dried at a temperature of 105°C for 3 h. Finally, the samples were sieved with 250 $\mu$m mesh size to obtain fine powder and was stored in plastic labelled bottles waiting for characterization.

*2.4. Adsorbent Characterization.* pH titration was adopted to evaluate the activated carbon surface charge [10–12]. 50 mg

dose of activated carbons was introduced in 50 mL of 0.01 M $KNO_3$ solution under varied pH conditions. The pH modification was achieved by drop additions of 0.1 M NaOH or 0.1 M HCl solution to obtained required pH. The adsorbent solutions in the flasks were then stirred for 48 h. The point of charge was determined by plotting the starting pH against changes in pH. FT-IR spectroscopy was used to study the surface functional groups (NICOLET iS 10, 2007, USA). The mixture of KBr to adsorbent was set at 1 : 10 mg. The samples were examined, and spectra in the region of 4000 to 400 $cm^{-1}$ were documented. X-ray diffractometer (Siemens) was used to assess crystalline phase (Model No.: 10190376, Germany). The scanning was conducted at a diffraction angle of ($2\theta$) with a range of 10° to 90°. The surface structure of the sorbent produced was characterized by FESEM (JEOL JSM-7100F Japan).

*2.5. Batch Adsorption Studies.* The adsorption studies were carried out in the batch process using 250 mL conical flasks at room temperature (25°C). 50 mL volumes of working adsorbate concentrations were prepared from acetic acid stock solution by dilution with double-distilled water to get the desired concentrations. The effect of initial adsorbate concentration (1, 1.25, 1.5, 1.7, and 2 M), adsorbent dose (0.1-0.8 g), and contact time (10-140min) was studied. The preferred mass of the adsorbent was measured using an electronic balance and transferred into a 250 mL conical flask containing 50 mL acetic acid. The contents were then agitated at a constant speed of 120 revolutions per min (rpm) for 120 min. At the end of each desired time, the samples were filtered in 0.22 filters to determine the concentration of the acetic acid left in the solution after the adsorption process had occurred. 10 mL of the filtrate was drawn and transferred into a clean conical flask; 2-3 drops of phenolphthalein indicator were added and then titrated with 0.1 M NaOH until the end point was attained. The process was repeated three times for every sample, and mean for residual concentration was then calculated. The removal percentage and adsorption capacity ($Q_e$) of acetic acid adsorbed by adsorbents were calculated by equations (1) and (2) below, respectively.

$$\text{Removal}\,(\%) = \frac{(C_o\text{-}C_e)}{C_o} \times 100, \tag{1}$$

$$Q_e = \frac{(C_o\text{-}C_e) \times v}{w}, \tag{2}$$

where $C_o$ (mg/L) is the initial concentration of acetic acid in solution and $C_e$ (mg/L) is the liquid concentration of acetic acid left in the solution after the adsorption process has occurred. $W$ is the mass of adsorbent (g), and $V$ is the volume of the solution (L).

## 3. Results and Discussions

*3.1. Point of Zero Charge ($pH_{pzc}$).* The point of zero charge results are shown in Figure 2(a), and the findings of study indicated that RH-AC and PP-AC had identical point of zero charge; thus, $pH_{pzc} = 6.8$. At this point, activated carbons are said to possess a net electrical neutral charge on surface. This implies that, as the pH of the solution decreases below pHpzc, the adsorbent surface gets protonated due to excessive competitiveness of hydrogen ion, promoting the adsorption of pollutants such as anions. So, if the pH of the solution is above pHpzc, hydroxide ions dominate in the solution resulting into deprotonation of the sorbent surface with negative charge, thereby favoring uptake of impurities such as cations [24]. $pH_{pzc}$ of the activated charcoal was almost equivalent to neutral point. Therefore, carbon samples were appropriate for the treatment of water containing acetic acid.

*3.2. X-Ray Diffraction.* Figure 2(b) shows the X-ray characteristics of the produced carbon materials. The findings demonstrate Bragg peak intensity in the $2\theta = 20\text{-}30°$ range for both activated carbons. The presence of the hump indicates a high level of disorder, which is an indicative characteristic of activated carbons. Additionally, the absence of a strong peak indicated that there were no identifiable minerals in the carbon materials produced [15]. Similar findings were also reported in literature by several researchers who successfully derived agro-based carbonaceous materials [14, 15].

*3.3. FT-IR Spectrum.* Figure 2(c) shows the findings of the surface functional group studies of the developed activated charcoal. The bands appearing at wave numbers 3743-3646 $cm^{-1}$ are associated with the bond vibration bound to -OH groups [25]. The absorption peaks at range 2336-2376 $cm^{-1}$ are related with the stretching vibration of C-O in carbon dioxide or carbon monoxide molecules. The peak seen 2180 $cm^{-1}$ is linked to bond stretching vibrations of alkynes (CC). Further, the bands noticed at (1673 and 1400) $cm^{-1}$ are connected to the benzene ring's bending vibration of C=C [26]. The wave number observed at the absorption band 1548 $cm^{-1}$ corresponds to the asymmetric and symmetric stretching of N-oxide functional group (N=O), whereas the band at 1052 $cm^{-1}$ is associated with antisymmetric stretch of C-O-C [27].

*3.4. FESEM Results.* FESEM micrographs were taken before adsorption of acetic acid and are shown in Figure 3. The micrographs indicated several cavities, high porous structure, and numerous interconnected pores that provide access to internal areas to adsorb acetate ions. The development of excellent surface characteristics of the produced activated carbons could be associated with chemical activation of the precursors at elevated temperatures (500°C) with the presence of an activating agent (40% $H_3PO_4$), resulting in the substantial elimination of volatile materials and stimulating the opening and formation of additional pores (micropores and mesopores) [20]. This also implies that the presence of cracks enhanced the surface area of the synthesized carbon. For the availability of the high porous structure, the findings indicate that the carbonaceous materials were effective for acetic acid removal in aqueous solution.

*3.5. Batch Adsorption Study*

*3.5.1. Effect of Contact Time.* Attainment of adsorption equilibrium depends on the contact time between the adsorbent

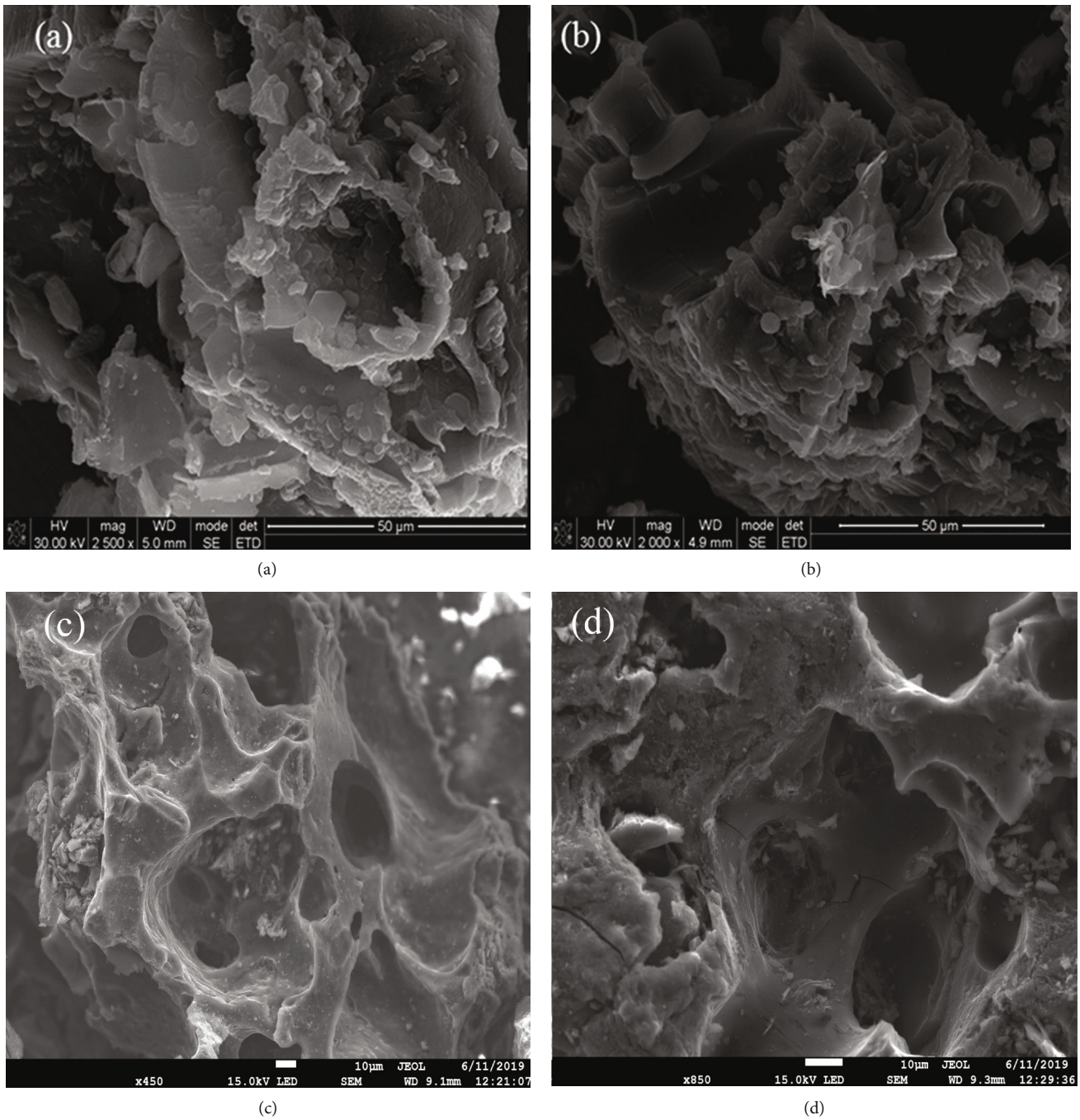


Figure 3: FESEM: (a, c) RH-AC and (b, d) PP-AC.

and adsorbate. In this study, the effect of contact time of adsorbate and adsorbent was examined and all other parameters were kept constant (i.e., agitation speeds of 120 rpm, dosage of 0.1 g/50 mL, and adsorbate concentration 0.6 M). The results in Figure 4(a) indicate that as the contact time increased, the adsorption capacity of acetic acid increased from 0.95 to 2.11 mg/g and 1.04 to 2.268 mg/g thus for PP-AC and RH-AC, respectively. This could be elucidated because as time was prolonged, more adsorbates were accommodated on the active sites of the adsorbents until equilibrium was attained [28]. This pattern of results was observed for 120 min; thereafter, a plateau was seen to appear, and no significant adsorption of acetic acid was noticed.

*3.5.2. Effect of Adsorbent Dosage.* The adsorbent dosage is among the important parameters in the optimization of the adsorption system. To evaluate the effect of adsorbent dose on adsorption, adsorbent dose ranging from 0.1 to 0.8 g with 50 mL adsorbate concentration 1.5 M and 120 min contact time with an agitation speed of 120 rpm were studied. The results obtained from this study are shown in Figure 4(b), which have demonstrated that increasing

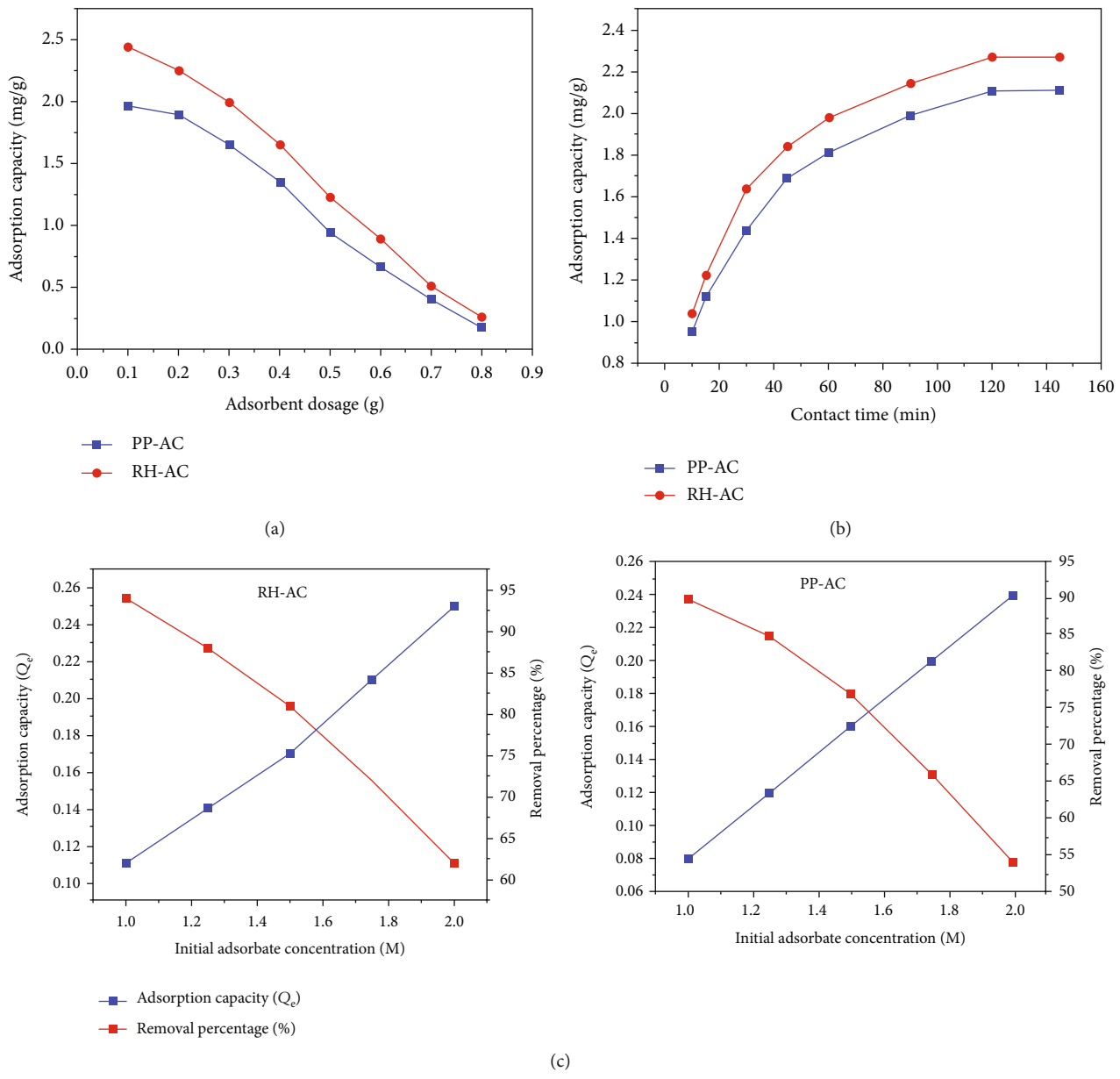


Figure 4: (a) The effect of contact time on acetic acid adsorption onto RH-AC and PP-AC, at contact time 90, initial concentration of 1.5 M, 0.1 g/50 mL, and agitation speed of 120 rpm. (b) The effect of adsorbent dosage on acetic acid adsorption onto RH-AC and PP-AC, contact time 90, initial concentration of 1.5 M, and agitation speed of 120 rpm. (c) The effect of adsorbate concentration on acetic acid adsorption onto RH-AC and PP-AC, contact time 120 min, adsorbent dose 0.1 g/50 mL, agitation speed of 120 rpm, and temperature.

adsorbent dosage for RH-AC decreased adsorption capacity from 2.44 to 0.25 mg/g. Likewise, increasing doses of PP-AC, the reduction in adsorption capacity of 1.98 to 0.18 mg/g was attained. The decrease in adsorption capacity as the dosage was increased could be associated with the fact that at high dosages, the available acetate ions are not enough to cover the present vacant sites on the adsorbents resulting into low adsorption capacity [1].

*3.5.3. Effect of Initial Adsorbate Concentration.* The influence of initial adsorbate concentration on the equilibrium adsorption capacity was also assessed, and the results for both adsorbents are displayed in Figure 4(c). The adsorption capacity for RH-AC increased from 0.11 to 0.25 mg/g, and the adsorption percentage decreased from 94 to 60% with an increase in initial adsorbate concentration. For similar initial concentrations, PP-AC the adsorption ability increased from 0.08 to 0.24 mg/g and adsorption percentage decreased from 90 to 54%. This visibly indicates that the mass gradient acts as a driving force for the adsorption process, and that the rise in adsorbate molecule concentration bulk in solution at constant adsorbent dose does boost the mass transfer process [29]. The reduction in percentage removal is due to the fact that at higher concentration, more acetate ions remain in the solution unadsorbed due to saturation of binding sites [30]. This occurs due to an increase in

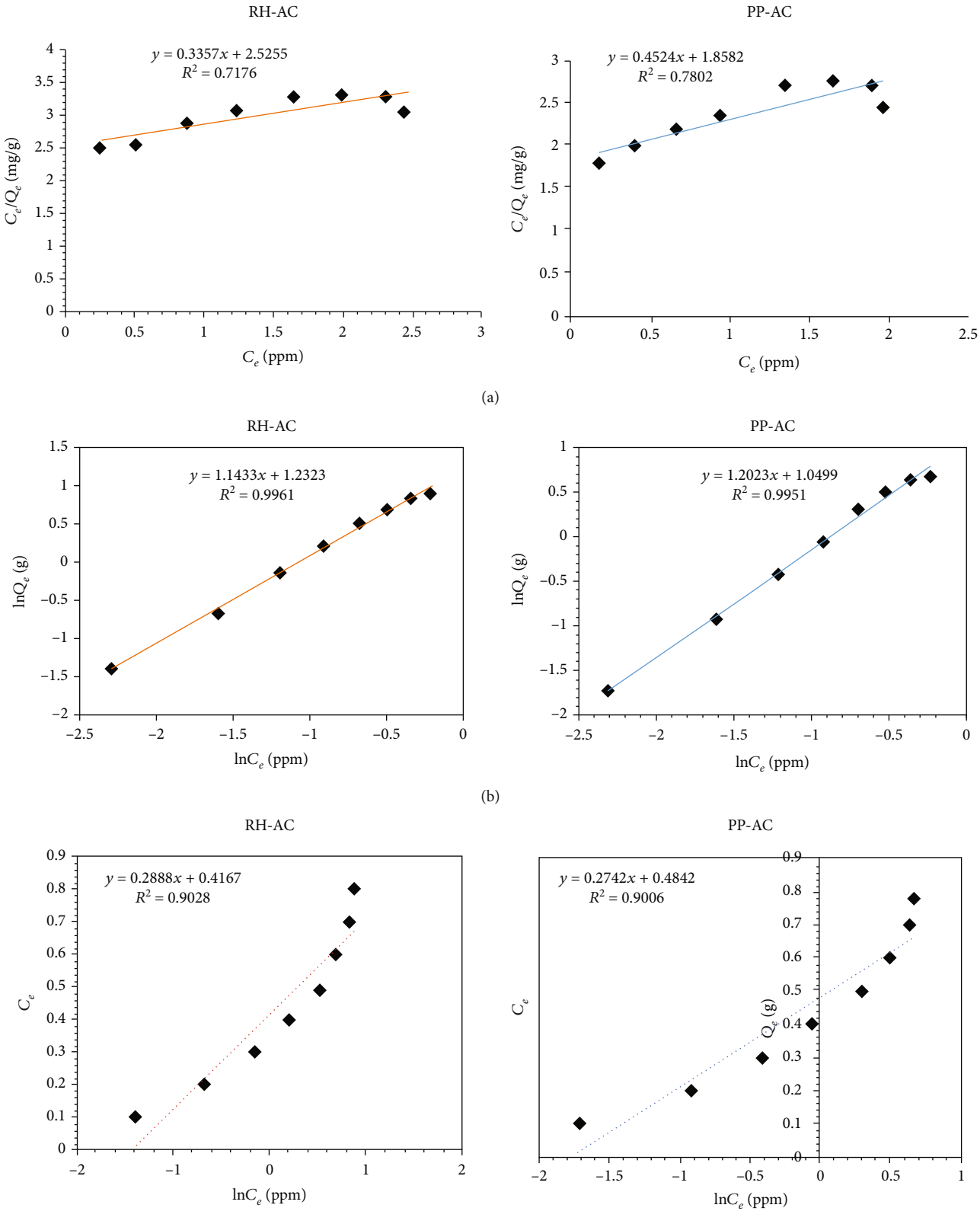


Figure 5: Continued.

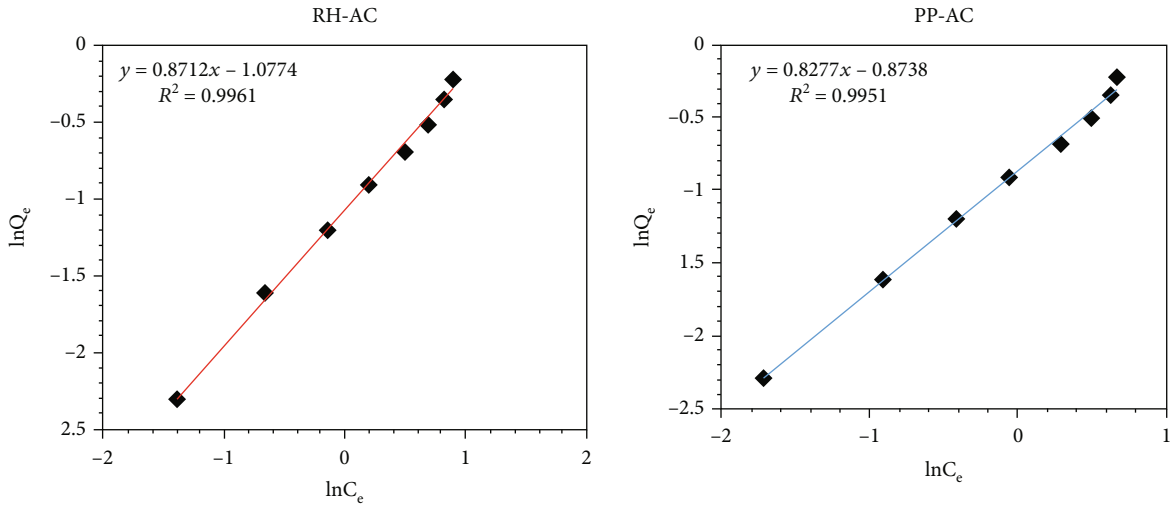


(d)

Figure 5: The (a) Langmuir, (b) Freundlich, (c) Temkin, and (d) Frenkel–Halsey–Hill for RH-AC and PP-AC, respectively.

Table 1: The Langmuir, Freundlich, Temkin, and isotherm model constants as well as correlation coefficients for acetic acid adsorption.

| | Freundlich | | |
|---|---|---|---|
| | $K_F$ (mg/g)(L.mg$^{-1}$)$^{1/n}$ | $n$ | $R^2$ |
| RH-AC | 3.4291 | 3.8747 | 0.9961 |
| PP-AC | 0.8317 | 2.8574 | 0.9951 |
| | Langmuir | | |
| | $q_m$ (mg/g) | $b$ (L.mg$^{-1}$) | $R^2$ |
| RH-AC | 2.9789 | 0.1329 | 0.7176 |
| PP-AC | 2.2104 | 0.2435 | 0.7802 |
| | Temkin | | |
| | $K_T$ (L/g) | $B$ (J/mol) | $R^2$ |
| RH-AC | 4.2328 | 0.2888 | 0.9028 |
| PP-AC | 5.8466 | 0.2742 | 0.9006 |
| | Frenkel–Halsey–Hill | | |
| | $K_H$ | $n$ | $R^2$ |
| RH-AC | 2.02 | 1.1478 | 0.9991 |
| PP-AC | 1.76 | 1.2082 | 0.9941 |

the number of ions competing for existing binding sites in the adsorbents. The increase in adsorption capacity with initial adsorbate concentration shows that the adsorbents (RH-AC and PP-AC) have a great affinity for acetic acid.

*3.6. Adsorption Isotherms.* Adsorption isotherms are mathematical models commonly used to describe the characteristics of the adsorption process between adsorbent and adsorbate phases when the adsorption equilibrium is achieved at a constant temperature. To appreciate the adsorption capacity of agro-based activated carbon prepared for the uptake of acetate ions from an aqueous solution, four isotherms, namely, Langmuir, Freundlich, Temkin, and Frenkel–Halsey–Hill were used to validate the data obtained in adsorption studies of acetic acid.

*3.6.1. Langmuir Isotherm.* The Langmuir mathematical isotherm model assumes that the adherence of the adsorbate to the adsorbent occurs on a homogenous surface by monolayer adsorption without any interaction between adsorbed molecules or ions. The linearized form of Langmuir's mathematical model is denoted by the following equation [31]:

$$\frac{C_e}{Q_e} = \frac{1}{bQ_m} + \frac{C_e}{Q_m}, \tag{3}$$

where $Q_e$ is the monolayer adsorption capacity of the adsorbent (mg/g), $C_e$ is the equilibrium concentration (mg/L), $Q_m$ is the maximum adsorption capacity that can be taken up per mass of adsorbent (mg/g), and $b$ (L/mg) is the Langmuir constant associated with the rate of sorption energy between adsorbate and adsorbent. The important characteristics of Langmuir isotherm can also be expressed in terms of a dimensionless constant separation factor or equilibrium parameter $R_{L,}$ which is explained as follows [32]:

$$R_L = \frac{1}{1 + bC_o}, \tag{4}$$

where $b$ is the Langmuir constant and $C_o$ is the initial concentration of acetic acid. The value of $R_L$ indicates the type of the isotherm to be either unfavorable ($R_L > 1$), linear ($R_L = 1$), favorable ($0 < R_L > 1$), or irreversible ($R_L = 0$) [33]. The constants of this model were calculated from the plot of $C_e$ versus $C_e/Q_e$ in Figure 5(a), and the values calculated are shown in Table 1.

*3.6.2. Freundlich Isotherm.* The Freundlich isotherm model is based on the assumption that the uptake of adsorbate occurs on a heterogeneous surface by monolayer adsorption

Table 2: Comparison of acetic acid adsorption on various adsorbent materials.

| Adsorbent | Temperature (K) | Initial concentration ($gL^{-1}$) | Adsorbent dose (g) | Adsorption capacity ($Q_m$ ($mg.g^{-1}$)) | Isotherm | Kinetic model | Reference |
|---|---|---|---|---|---|---|---|
| Hydrotalcites | 303 | - | - | 91.39-125.65 | Freundlich | Pseudosecond-order | [39] |
| Zeolite | 308 | 11.8-71.8 | 5 | 405.5 | Freundlich | Pseudosecond-order | [37] |
| Activated carbon | 300 | 0.42-23.7 | 0.1 | 55.2-939.8 | Temkin, Freundlich | - | [40] |
| Hydrotalcite MG7Oc | 323 | 1.0-7.0 | 0.036 | 145.3 | Sips | - | [41] |
| Ion-exchange resin | 308 | 0.15-0.25 | - | 405.5 | Langmuir | Pseudosecond-order | [42] |
| Metal organic frame works nanotubes | 298 | 9.9-30.4 | 0.10 | 270.5 | Freundlich | Pseudo-second-order | [43] |
| Multiwall carbon nanotubes | 298 | 0.037-0.117 | 0.02 | 5.7 | Langmuir | Pseudo-second-order | [44] |
| SB-AC | 305 | 0.2-1.0 | 0.4 | 0.661-4.56 | Dubinin-Radushkevich | Pseudo-second-order | [1] |
| Fly ash | 298 | 0.05-1.0 | 5-50 | 7.00 | Langmuir | Pseudosecond-order | [45] |
| FA-CAC | 304 | 600-6000 | 12-28 | 21.9-71.6 | Freundlich, Langmuir | Pseudofirst-order | [2] |
| RH-AC | 298 | 1.0-2.0 | 0.1 | 0.11-0.25 | Freundlich, Frenkel–Halsey–Hill | Pseudosecond order | This study |
| PP-AC | 298 | 1.0-2.0 | 0.1 | 0.08-0.24 | Freundlich, Frenkel–Halsey–Hill | Pseudosecond-order | This study |

[34]. The linear equation of this isotherm can be written as follows.

$$\log Q_e = \log K_f + \frac{1}{n} \log C_e, \tag{5}$$

where $K_f$ ((mg/g) $(L/g)^{1/n}$) and $n$ are the Freundlich constants that are connected with the adsorption capacity and intensity, respectively. The coefficients of this mathematical model were calculated from the intercept and slope of the linear plot of $\log C_e$ versus $\log Q_e$ in Figure 5(b). The values attained are listed in Table 1.

*3.6.3. Temkin Isotherm.* Temkin isotherm model postulates that because of indirect adsorbate/sorbate interactions, the heat of adsorption of the atoms adsorbed would linearly decrease with coverage. It also suggests that the adsorption process is characterized by a uniform distribution of binding energies at the adsorbent surface [35]. The Temkin isotherm linearized equation is given as equation (6) below:

$$Q_e = B \ln K_T + B \ln C_e. \tag{6}$$

$B = RT/b$, where $K_T$ is the Temkin equilibrium binding constant in (L/mg), corresponding to the maximum binding energy and the constant $B$ is associated with the heat of adsorption. $T$ and $K$ are the absolute temperature (k) and the universal gas constant ($8.314\,J{\cdot}mol^{-1}{\cdot}K^{-1}$), respectively. The values of Temkin constants $K_T$ and $B$ are calculated from the intercept and slope of the linear plots of $Q_e$ versus $\ln C_e$ in Figure 5(c), and the results are shown in Table 1.

*3.6.4. Frenkel–Halsey–Hill Isotherm.* This model is suitable for multilayer adsorption and heteroporous adsorbents. The Halsey adsorption isotherm in linear form is signified as per the equation below [36]:

$$\ln Q_e = \frac{1}{n} \ln K_H - \frac{1}{n} \ln C_e, \tag{7}$$

where $Q_e$ is the quantity of adsorption at equilibrium and $C_e$ is the adsorbate concentration at equilibrium. $K_H$ and $n$ are Halsey's isotherm constants and are calculated from the slope and intercept of the plot $\ln Q_e$ versus $\ln C_e$ in Figure 5(d) with attained results are displayed in Table 1.

From Table 1, in terms of correlation coefficient ($R^2$) values obtained from the four isotherm models, the applicability of the isotherms is ranked in the order (Freundlich=-Frenkel–Halsey–Hill)>Temkin>Langmuir. The best fit is attained by Freundlich and Frenkel–Halsey–Hill isotherms with (all values of $R^2 > 0.99$) for both adsorbents suggesting the applicability of these isotherms in fitting the experimental data over other tested mathematical models under similar

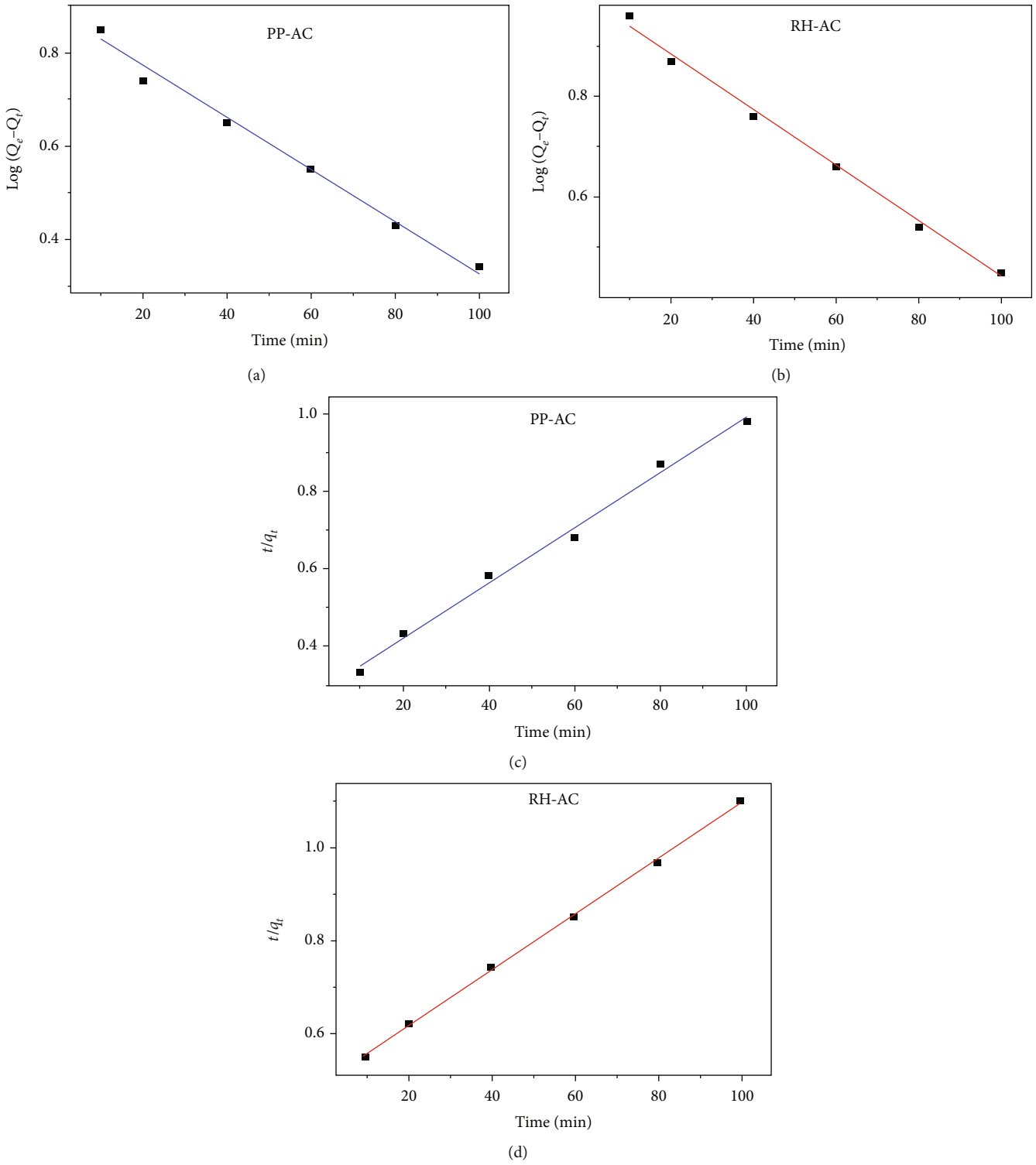


Figure 6: The plot of (a, b) pseudofirst-order and (c, d) pseudosecond-order.

conditions. The results indicate that the adsorption of acetic acid followed a multilayer through the existence of a heterogeneous pore distribution in the adsorbent surface as Freundlich and Frenkel–Halsey–Hill isotherm postulations imply [36]. Furthermore, the efficacious fitting of the experimental data by Frenkel–Halsey–Hill model also confirms that the adsorbents were heteroporous in nature. Similar observations were also reported in different studies for adsorption of acetic acid from aqueous solution using zeolite [37]. Table 2 provides the summary of the main results attained in the study and those reported in literature.

*3.7. Kinetic Models.* Two kinetic models, namely, pseudofirst-order and pseudosecond-order, were used to

Table 3: The plot of pseudofirst-order and pseudosecond-order model parameters.

| | Pseudofirst-order | | | |
|---|---|---|---|---|
| | $K_1$ (min$^{-1}$) | $Q_e$ (mg/g) | $R^2$ | SSE |
| RH-AC | 0.0122 | $2.67 \times 10^{-2}$ | 0.9680 | 0.0423 |
| PP-AC | 0.0212 | $3.54 \times 10^{-2}$ | 0.9282 | 0.0642 |
| | Pseudosecond-order | | | |
| | $Q_e$ (mg/g) | $K_2$ (mg/gmin) | $R^2$ | SSE |
| RH-AC | 0.199 | 35.08 | 0.9918 | 0.0126 |
| PP-AC | 0.187 | 30.88 | 0.9943 | 0.0237 |

identify the adsorption process. The linear equations of first-order were elucidated using the equation below [38]:

$$\ln (q_e - q_t) = (q_e - k_1 t), \tag{8}$$

where $q_e$ (mg/g) and $q_t$ (t) are the adsorption abilities at equilibrium and at the time, respectively, and $k_1$ (min$^{-1}$) is the rate constant. The values of $k_1$ and $q_e$ were determined from the slope and intercept of the plots $\ln (q_e - q_t)$ versus $t$, respectively, in Figures 6(a) and 6(b). The linearized form of second-order can be written as follows [26]:

$$\frac{1}{q_e} = \frac{1}{k_2 q^2} + \frac{1}{q_e} t, \tag{9}$$

where $k_2$ (g/mg/min) is the main rate constant of pseudosecond-order adsorption. The values of $k_2$ and $q_e$ are calculated from the slope and intercept of the linear plots $t/q_t$ against $t$, in Figures 6(c) and 6(d). The results obtained for both kinetic models are shown in Table 3. The regression coefficients obtained for pseudosecond-order were higher for both adsorbents (RH-AC and PP-AC) compared to those of pseudofirst-order. This means that the adsorption data conforms to this kinetic model, which is an indication that the rate-limiting reaction of the acetic acid adsorption process was chemisorption dealing with valence force through electron sharing [20]. The applicability of kinetic models is confirmed through the sum of error squares as given by the following:

$$\text{SSE\%} = \frac{\sqrt{\sum \left(Q_{e,\text{cal}} - Q_{e,\text{exp}}\right) 2}}{N}, \tag{10}$$

where $N$ is the number of data points. The $R^2$ values which resulted from the linear plot were > 0.99 for both adsorbents. The higher $R^2$ value and lower value of SSE shown in Table 3 for the calculated for pseudosecond-order indicates a better fit, and that the adsorption process followed pseudosecond-order kinetic model. Similar findings were also reported by [35].

The maximum adsorption capacity for the adsorption of acetic acid by RH-AC and PP-AC adsorbents was found to be 0.25 mg/g and 0.24 mg/g, respectively.

*3.8. Regeneration and Reusability.* Regeneration studies were carried out to determine the suitability of the derived adsorbents in practical applications and the economic possibility of the adsorption process. The alkaline 0.1 M sodium hydroxide and distilled water were selected and used as desorbing agents. 0.2 g of the adsorbents was transferred into a 250 mL conical flask containing 1.5 M acetic acid which was agitated at 120 rpm for 90 min to adsorb acetic acid. The adsorbents were separated from the acids and then washed with sodium hydroxide using a magnetic stirrer for 10 min to remove physically adsorbed acetic acid followed by distilled water and finally oven-dried at 105°C for 2 h. The adsorbents were then utilized in the next cycle of adsorption studies. The above process was repeated for four times, and a very slight change was observed.

## 4. Conclusion

The current study has found out that activated carbons prepared were effective for acetic acid removal. The activated carbons had the same point of zero charge, many functional groups were excellent for adsorption, and they were amorphous, thus according to the characterization studies. Increases in contact time, adsorbate concentration, and adsorbent dosage improved the removal of acetic acids. The adsorption data followed two isotherms, namely, Freundlich and Frenkel–Halsey–Hill while kinetic data conformed to pseudosecond-order models. Reusability tests revealed that the adsorbents may be reused numerous times without losing their adsorbing affinity, thus allowing for multiple uses.

## Data Availability

Data for this paper has been included in the manuscript and is available upon request to the corresponding author.

## Conflicts of Interest

The authors do solemnly declare that there is no any conflict of interest as the research was not conducted for commercial or financial purposes.

## Acknowledgments

The authors acknowledge EXCEED/Swindon and German Academic Exchange Service (DAAD) for technical and financial support. The authors are also grateful to Professor W.L. Masamba of BIUST for his assistance in sample characterization. The final vote of thanks should go to Jaramogi Oginga Odinga University of Science and Technology in Kenya, for allowing us to use their laboratory.

## References

[1] F. A. Adekola and I. A. Oba, "Biosorption of formic and acetic acids from aqueous solution using activated carbon from shea butter seed shells," *Applied Water Science*, vol. 7, no. 6, pp. 2727–2736, 2017.

[2] N. Kannan and A. Xavier, "New composite mixed adsorbents for the removal of acetic acid by adsorption from aqueous solutions-a comparative study," *Toxicological and Environmental Chemistry*, vol. 79, no. 1–2, pp. 95–107, 2001.

[3] M. E. Goher, A. M. Hassan, I. A. Abdel-Moniem, A. H. Fahmy, M. H. Abdo, and S. M. El-sayed, "Removal of aluminum, iron and manganese ions from industrial wastes using granular activated carbon and Amberlite IR-120H," *Egyptian Journal of Aquatic Research*, vol. 41, no. 2, pp. 155–164, 2015.

[4] S. Nurani, H. Abdul, and W. Lau, "Detection of contaminants in water supply: a review on state-of-the-art monitoring technologies and their applications," *Sensors Actuators B: Chemical*, vol. 255, pp. 2657–2689, 2018.

[5] A. F. Freitas, M. F. Mendes, and G. L. V. Coelho, "Thermodynamic study of fatty acids adsorption on different adsorbents," *Journal of Chemical Thermodynamics*, vol. 39, no. 7, pp. 1027–1037, 2007.

[6] S. Somma, E. Reverchon, and L. Baldino, "Water purification of classical and emerging organic pollutants: an extensive review," *ChemEngineering*, vol. 5, no. 3, p. 47, 2021.

[7] A. Ojstršek, P. Vouk, and D. Fakin, "Adsorption of pollutants from colored wastewaters after natural wool dyeing," *Materials*, vol. 15, no. 4, p. 1488, 2022.

[8] E. Vunain, J. B. Njewa, T. T. Biswick, and A. K. Ipadeola, "Adsorption of chromium ions from tannery effluents onto activated carbon prepared from rice husk and potato peel by H3PO4 activation," *Applied Water Science*, vol. 11, no. 9, pp. 1–14, 2021.

[9] I. Ivancev-Tumbas, L. Landwehrkamp, R. Hobby, M. Vernillo, and S. Panglisch, "Adsorption of organic pollutants from the aqueous phase using graphite as a model adsorbent," *Adsorption Science and Technology*, vol. 38, no. 7–8, pp. 286–303, 2020.

[10] M. S. Reza, C. C. Yun, S. Afroze et al., "Preparation of activated carbon from biomass and its' applications in water and gas purification, a review," *Arab Journal of Basic and Applied Science*, vol. 27, no. 1, pp. 208–238, 2020.

[11] F. A. Al-khaldi, B. Abu-sharkh, A. Mahmoud, M. Imran, T. Laoui, and M. Ali, "Effect of acid modification on adsorption of hexavalent chromium (Cr (VI)) from aqueous solution by activated carbon and carbon nanotubes," *Desalination Water and Treatment*, vol. 57, article 1021847, pp. 7232–7244, 2015.

[12] R. Yavuz, I. Orbak, and N. Karatepe, "Factors affecting the adsorption of chromium (VI) on activated carbon," *Journal Environmental Science and Health- Part A*, vol. 41, no. 9, pp. 1967–1980, 2006.

[13] M. Blachnio, A. Derylo-Marczewska, B. Charmas, M. Zienkiewicz-Strzalka, V. Bogatyrov, and M. Galaburda, "Activated carbon from agricultural wastes for adsorption of organic pollutant," *Molecules*, vol. 25, no. 21, 2020.

[14] T. Mkungunugwa, S. Manhokwe, A. Chawafambira, and M. Shumba, "Synthesis and characterisation of activated carbon obtained from Marula (*Sclerocarya birrea*) nutshell," *Journal of Chemistry*, vol. 2021, Article ID 5552224, 9 pages, 2021.

[15] E. Vunain and T. Biswick, "Adsorptive removal of methylene blue from aqueous solution on activated carbon prepared from Malawian baobab fruit shell wastes : equilibrium , kinetics and thermodynamic studies and thermodynamic studies," *Separation Science and Technology*, vol. 1–15, 2018.

[16] S. Hosseini, S. Masoudi Soltani, H. Jahangirian, F. Eghbali Babadi, T. S. Y. Choong, and N. Khodapanah, "Fabrication and characterization porous carbon rod-shaped from almond natural fibers for environmental applications," *Journal of Environmental Chemical Engineering*, vol. 3, no. 4, pp. 2273–2280, 2015.

[17] J. B. Njewa, E. Vunain, and T. Biswick, "Synthesis and characterization of activated carbons prepared from agro-wastes by chemical activation," *Journal of Chemistry*, vol. 2022, Article ID 9975444, 13 pages, 2022.

[18] S. Joshi and B. Pokharel, "Preparation and characterization of activated carbon from Lapsi *(Choerospondias axillaris*) seed stone by chemical activation with potassium hydroxide," *Journal of Institute of Engineering*, vol. 9, no. 1, pp. 79–88, 2014.

[19] W. Tathongpat, J. Taweekun, and K. Maliwan, "Synthesis and characterization of microporous activated carbon from rubberwood by chemical activation with KOH," *Carbon Letters*, vol. 31, no. 5, pp. 1079–1088, 2021.

[20] E. Vunain, D. Kenneth, and T. Biswick, "Synthesis and characterization of low-cost activated carbon prepared from Malawian baobab fruit shells by $H_3PO_4$ activation for removal of Cu(II) ions: equilibrium and kinetics studies," *Applied Water Science*, vol. 7, no. 8, pp. 4301–4319, 2017.

[21] Y. Li, X. Zhang, R. Yang, G. Li, and C. Hu, "The role of $H_3PO_4$ in the preparation of activated carbon from NaOH-treated rice husk residue," *RSC Advances*, vol. 5, no. 41, pp. 32626–32636, 2015.

[22] P. Ravichandran, P. Sugumaran, S. Seshadri, and A. H. Basta, "Optimizing the route for production of activated carbon from Casuarina equisetifolia fruit waste," *Royal Socety of Chemsitry*, vol. 5, no. 7, 2018.

[23] J. Zhao, L. Yu, F. Zhou, H. Ma, K. Yang, and G. Wu, "Synthesis and characterization of activated carbon from sugar beet residue for the adsorption of hexavalent chromium in aqueous solutions," *Royal Socety of Chemsitry*, vol. 11, no. 14, pp. 8025–8032, 2021.

[24] D. Lataye, D. Malwade, V. Kurwadkar, S. Mhaisalkar, and D. Ramirez, "Adsorption of hexavalent chromium onto activated carbon derived from Leucaena leucocephala waste sawdust : kinetics , equilibrium and thermodynamics," *International journal of Environmental Science and Technology*, vol. 13, no. 9, pp. 2107–2116, 2016.

[25] N. S. Barot and H. K. Bagla, "Eco-friendly waste water treatment by cow dung powder (adsorption studies of Cr (III), Cr (VI) and Cd (II) using tracer technique)," *Desalination Water and Treatment*, vol. 38, no. 1-3, pp. 104–113, 2012.

[26] T. Benzaoui, A. Selatnia, and D. Djabali, "Adsorption of copper (II) ions from aqueous solution using bottom ash of expired drugs incineration," *Adsorption Science and Technology*, vol. 36, no. 1-2, pp. 114–129, 2018.

[27] R. Labied, O. Benturki, A. Hamitouche, and A. Donnot, "Adsorption of hexavalent chromium by activated carbon obtained from a waste lignocellulosic material (Ziziphus jujuba cores): kinetic , equilibrium , and thermodynamic study," *Adsorption Science and Technology*, vol. 38, pp. 1066–1099, 2018.

[28] A. S. Yusuff, "Adsorption of hexavalent chromium from aqueous solution by *Leucaena leucocephala* seed pod activated carbon : equilibrium, kinetic and thermodynamic studies," *Arab Journal of Basic and Applied Sciences*, vol. 26, no. 1, pp. 89–102, 2019.

[29] V. O. Shikuku, R. Zanella, C. O. Kowenje, F. F. Donato, N. M. G. Bandeira, and O. D. Prestes, "Single and binary adsorption of sulfonamide antibiotics onto iron - modified clay : linear

and nonlinear isotherms, kinetics, thermodynamics, and mechanistic studies," *Applied Water Science*, vol. 8, no. 6, pp. 1–12, 2018.

[30] S. Zafar, M. I. Khan, M. H. Lashari et al., "Removal of copper ions from aqueous solution using NaOH-treated rice husk," *Emergent Materials*, vol. 3, no. 6, pp. 857–870, 2020.

[31] A. B. Mandal, S. Nethaji, and A. Sivasamy, "Adsorption isotherms, kinetics and mechanism for the adsorption of cationic and anionic dyes onto carbonaceous particles prepared from *Juglans regia* shell biomass," *International Journal of Environment Science and Technology*, vol. 10, no. 2, pp. 231–242, 2013.

[32] M. K. Rai, B. S. Giri, Y. Nath et al., "Adsorption of hexavalent chromium from aqueous solution by activated carbon prepared from almond shell: kinetics, equilibrium and thermodynamics study," *Journal of Water Supply:Research and Technology*, vol. 67, no. 8, pp. 724–737, 2018.

[33] I. Demiral, F. Tumsek, B. Karabacako, and H. Demiral, "Adsorption of chromium (VI) from aqueous solution by activated carbon derived from olive bagasse and applicability of different adsorption models," *Chemical Engineering Journal*, vol. 144, no. 2, pp. 188–196, 2008.

[34] B. H. Hameed, D. K. Mahmoud, and A. L. Ahmad, "Equilibrium modeling and kinetic studies on the adsorption of basic dye by a low-cost adsorbent : coconut (*Cocos nucifera*) bunch waste," *Journal of Hazardous Materials*, vol. 158, no. 1, pp. 65–72, 2008.

[35] E. Vunain, D. Houndedjihou, M. Monjerezi, A. A. Muleja, and B. T. Kodom, "Adsorption, kinetics and equilibrium studies on removal of catechol and resorcinol from aqueous solution using low-cost activated carbon prepared from sunflower (*Helianthus annuus*) Seed Hull Residues," *Water Air and Soil Pollution*, vol. 229, no. 11, p. 366, 2018.

[36] M. T. Amin, A. A. Alazba, and M. Shafiq, "Adsorptive removal of reactive black 5 from wastewater using bentonite clay: isotherms, kinetics and thermodynamics," *Sustainability*, vol. 7, no. 11, pp. 15302–15318, 2015.

[37] H. Zhang, Y. Wang, P. Bai, X. Guo, and X. Ni, "Adsorptive separation of acetic acid from dilute aqueous solutions : adsorption kinetic , isotherms , and thermodynamic studies," *Journal of Chemical Engineering*, vol. 61, no. 1, pp. 213–219, 2016.

[38] S. Islam, B. C. Ang, S. Gharehkhani, A. Binti, and M. Afifi, "Adsorption capability of activated carbon synthesized from coconut shell," *Carbon Letters*, vol. 20, pp. 1–9, 2016.

[39] B. Travalia and S. Forte, "New proposal in a biorefinery context: recovery of acetic and formic acids by adsorption on hydrotalcites," *Journal of Chemical Engineering and Data*, vol. 65, no. 9, pp. 4503–4511, 2020.

[40] D. J. D. Dina, A. R. Ntieche, J. N. Ndi, and J. Ketcha Mbadcam, "Adsorption of acetic acid onto activated carbons obtained from maize cobs by chemical activation with zinc chloride ($ZnCl_2$)," *Research Journal of Chemical Sciences*, vol. 2, no. 9, pp. 42–49, 2012.

[41] B. J. Liu, Z. J. Hu, and Q. L. Ren, "Single-component and competitive adsorption of levulinic/formic acids on basic polymeric adsorbents," *Colloids Surfaces A Physicochemical and Engineering Aspects*, vol. 339, no. 1–3, pp. 185–191, 2009.

[42] H. Lv, Y. Sun, M. Zhang, Z. Geng, and M. Ren, "Removal of acetic acid from fuel ethanol using ion-exchange resin," *Energy and Fuels*, vol. 26, no. 12, pp. 7299–7307, 2012.

[43] H. Zhang, X. Lan, P. Bai, and X. Guo, "Adsorptive removal of acetic acid from water with metal-organic frameworks," *Chemical Engineering Reseatch and Design*, vol. 111, pp. 127–137, 2016.

[44] Ö. Özcan, I. Inci, and Y. S. Aşçi, "Multiwall carbon nanotube for adsorption of acetic acid," *Journal of Chemical Engineering and Data*, vol. 58, no. 3, pp. 583–587, 2013.

[45] H. Zeidan, D. Ozdemir, N. Kose, E. Pehlivan, G. Ahmetli, and M. E. Marti, "Separation of formic acid and acetic acid from aqueous solutions using sugar beet processing fly ash : characterization, kinetics, isotherms and thermodynamics," *Desalination and Water Treatment*, vol. 202, pp. 283–294, 2020.